Bioconjugate Chemistry

Article

pubs.acs.org/bc

Design, Synthesis, and Therapeutic Evaluation of Poly(acrylic acid)−tetraDOCA Conjugate as a Bile Acid Transporter Inhibitor

Jooho Park,[†] Taslim A. Al-Hilal,[†,‡] Jee-Heon Jeong,[§] Jeong uk Choi,[†] and Youngro Byun*[,†,¶]

[†]Research Institute of Pharmaceutical Sciences, College of Pharmacy, and [¶]Department of Molecular Medicine and Biopharmaceutical Sciences, Graduate School of Convergence Science and Technology, Seoul National University, Seoul 151-742, South Korea

[‡]Center for Theragnosis, Biomedical Research Institute, Korea Institute of Science and Technology, Seoul 136-791, South Korea

[§]College of Pharmacy, Yeungnam University, Gyeongsan 712-749, South Korea

Supporting Information

ABSTRACT: Regulation of cholesterol and bile acid homeostasis has been attracting attention as a pharmaceutical target for the treatment of diseases, such as hypercholesterolaemia and type 2 diabetes. In recent years, small bile acid analogues have been developed for the purpose of apical sodium-dependent bile acid transporter (ASBT) inhibition. Here, we designed a novel hydrophilic ASBT inhibitor using oligomeric bile acid with a high affinity with ASBT. Polyacrylic acid−tetraDOCA conjugates (PATD) have the ability to bind to ASBT in order to induce hypocholesterolemic effects. Both the viability and the functionality of PATD were evaluated in vitro, showing that PATDs were effective in inhibiting the increases of cholesterol in the blood and oil in the liver induced by high fat diet (HFD). The results indicated that the newly developed biomaterials with oligomeric bile acids and a hydrophilic polymer are potent therapeutic agents for hyperlipidemia.

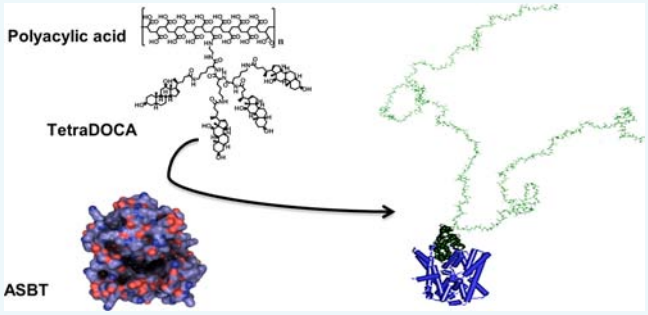

INTRODUCTION

Hyperlipidemia is a major risk factor for atherosclerosis and cardiovascular diseases.[1−3] Hyperlipidemia includes hypercholesterolemia and hypertriglyceridemia, which were shown to increase levels of cholesterol and triglycerides in the blood. Recently, the inhibition of cholesterol homeostasis and intestinal absorption of bile acids has attracted attention as a pharmacological target for the hypocholesterolemic effect, which is necessary for the treatment of hypercholesterolaemia.[4] The regulation of cholesterol and bile acid homeostasis is important, because about 50% of cholesterol is eliminated from the body by converting into bile acid.[5] Bile acids, which are synthesized from cholesterol in the liver and released from the gallbladder into the small intestine, are constantly reabsorbed and recycled in the enterohepatic circulation.[6,7]

Cholesterol-derived amphipathic bile acids are released from the bile duct, and more than 90% of released bile acids are then reabsorbed in the ileum by the apical sodium-dependent bile acid transporter (ASBT, also known as SLC10A2).[8] For this reason, ASBT is considered a pharmaceutical target for the treatment of hypercholesterolaemia, cholestatic liver disease, and type 2 diabetes.[9,10] Small synthetic ASBT inhibitors have shown considerably lower plasma cholesterol levels in animal models.[11,12] Moreover, ASBT inhibitors have been shown to increase the conversion of hepatic cholesterol into bile acids in the liver when they inhibit the recycling of bile acid in the enterohepatic circulation.[13]

Bile acid analogues, which are small hydrophobic synthetic molecules with steroid nucleus or nonsteroid structure, have considerable therapeutic potential related to the biological function of bile acid.[14,15] In recent years, the development of bile acid analogues has shown progress with regard to the molecular structure of bile acids and the bile acid-binding domains of bile acid transporter and receptor.[16−18] They have bile acid-similar structures to fit into a tight bile acid binding pocket of the targets.[16] Obeticholic acid and synthetic bile acid receptor agonists are also currently being investigated in phase II and phase III trials in patients.[19−21] Because of the small molecular size and hydrophobicity of bile acid mimics, they are usually absorbed in the GI tract and inhibit the bile acid receptors or transporters which exist in the intestine, liver, bile duct, and kidney.[16] However, bile acid receptors control a number of fundamental pathways in the liver and physiological processes including energy metabolism, glucose homeostasis, and inflammation; these are essential for normal living and digestion.[22−28] These various bile acid receptor actions could complicate bile acid based drug development and cause unexpected effects in a long-term drug administration.[16]

Unlike bile acid receptors in the liver, bile acid transporters in the ileum are much more attractive pharmaceutical targets.

Received: April 22, 2015
Revised: June 16, 2015
Published: June 18, 2015

DOI: 10.1021/acs.bioconjchem.5b00230
Bioconjugate Chem. 2015, 26, 1597−1605

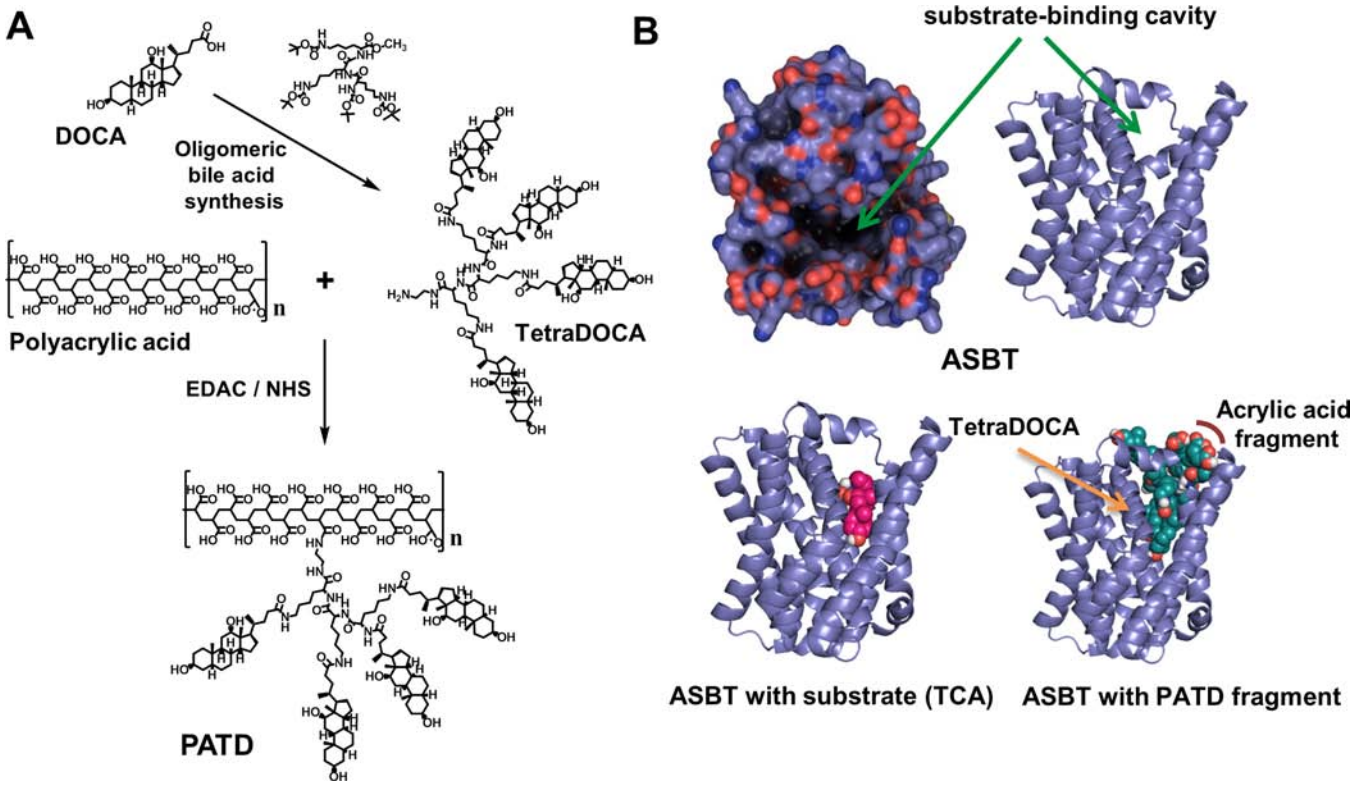

Figure 1. (A) Schematic synthesis protocol and molecular structures showing poly(acrylic acid), tetraDOCA, and poly(acrylic acid)−tetraDOCA conjugate (PATD). (B) In silico molecular docking of taurocholic acid (TCA) and poly(acrylic acid)−tetraDOCA conjugate (PATD) within the substrate-binding site of apical sodium-dependent bile acid transporter (ASBT) model. The substrate-binding cavity in ASBT is open to the cytoplasm.

When the therapeutic materials focus on the bile acid in the ileum, extensive drug metabolism and receptor interaction can be avoided. That is why GlaxoSmithKline recently tried to develop a synthetic nonabsorbable ASBT inhibitor for the treatment of type 2 diabetes.[29,30] Current drug development strategy based on the use of bile acid prefers to inhibit the transporters in the distal ileum which is the primary site of ASBT.

Conjugating a polymer could be an attractive approach to optimize the physical and chemical properties of biomaterials and make them useful materials as therapeutic agents.[31−34] Minimizing the systemic side effects and developing non-systemic bile acid based polymer targeting the bile acid transporter in the ileum will provide a promising strategy for drug development.[4,35,36] Here, we introduce a novel ASBT inhibitor using nonabsorbable hydrophilic polymer and oligomeric bile acid which has a high affinity to ASBT. In our previous study, we developed bile acid-based oligomers which showed selectivity for ASBT using multiple deoxycholic acids.[37−39] In this study, we designed and confirmed the activity of poly(acrylic acid)−tetraDOCA conjugate (PATD) as a bile acid transporter inhibitor. We also evaluated the therapeutic effect of PATD in a preclinical animal model of hyperlipidemia. This study could be discussed in terms of first macromolecule-based drug development for ASBT inhibition using a polymer and natural bile acids.

RESULTS AND DISCUSSION

Synthesis and Characterization of Polyacrylic Acid−tetraDOCA Conjugate. ASBT inhibitors have been clinically explored as lipid-lowering agents for the treatment of hypercholesterolaemia, cholestatic liver disease, and type 2 diabetes mellitus.[9] Numerous small steroidal and nonsteroidal compounds have been designed and synthesized for ASBT inhibition. In the presented study, we prepared novel ASBT inhibitors by conjugating poly(acrylic acid) with different ratios of tetraDOCA. TetraDOCA was chemically conjugated to poly(acrylic acid) by amide coupling reaction. The molecular structures of PATDs are shown in Figure 1 and characterization of these molecules was described in Table 1. We planned to synthesize products which have conjugation ratio ranging from 1 to 5. After synthesis, the molecular coupling ratios of PATD1 and PATD3 were 1.1 and 3.2, respectively.

Table 1. Synthesis, Characterization, and Dissociation Rate Constants (K_D) of Polyacrylic Acid−tetraDOCA Conjugate (PATD) Using Sulfuric Acid and SPR Study[a]

materials	conjugation ratio[b]	feed mole ratio (TetraDOCA)	feed mole ratio (EDAC/NHS)	avg. MW (kDa)	K_D[c] (nM) to ASBT
TCA	--	--	--	0.5	120.7
PATD1	1.10 ± 0.03	3	20	102	39.1
PATD3	3.24 ± 0.04	10	50	106	1.5

[a]Results are the means ± standard deviation. [b]Conjugation ratio of tetraDOCA and poly(acrylic acid) (1) measured using sulfuric acid assay. [c]Calculated by SPR software.

To figure out the interaction between PATD and ASBT, we measured its dissociation rate constants at equilibrium (K_D) using surface plasmon resonance (SPR). The affinity analysis was performed using BIAcore T100 evaluation software.

DOI: 10.1021/acs.bioconjchem.5b00230
Bioconjugate Chem. 2015, 26, 1597−1605

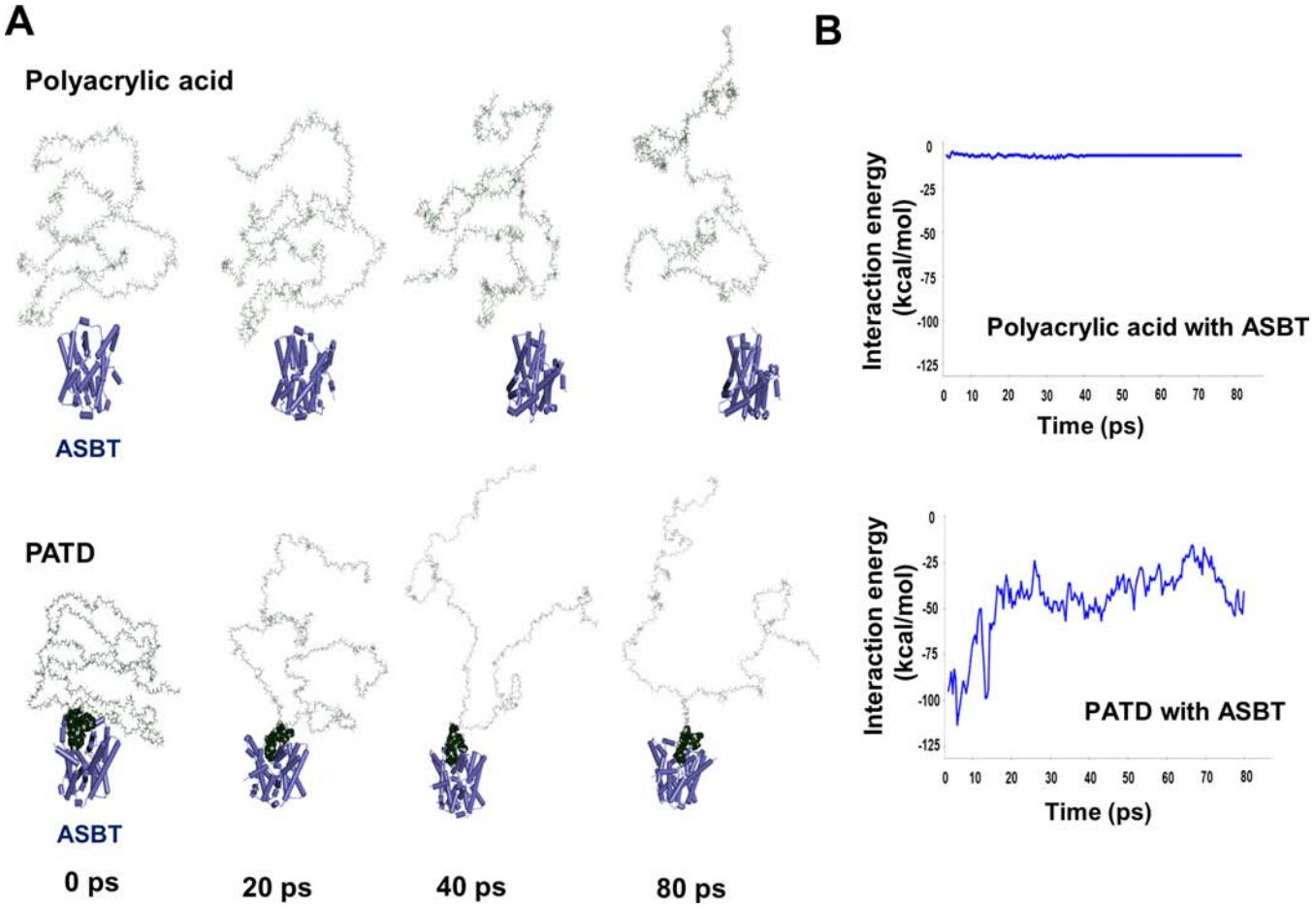

Figure 2. (A) Molecular dynamic simulation of PATD and ASBT (B) Comparsion of the interaction energy between ASBT and poly(acrylic acid) or PATD. The binding interaction of the PATD-ASBT complex was maintained during MD simulation.

Sodium taurocholate (TCA) which is the original substrate of ASBT was also used for SPR study. PATD1 (K_D = 39.1 nM) and PATD3 (K_D = 1.5 nM) had a higher binding affinity to ASBT than that of TCA (K_D = 120.7 nM) (Table 1). This explains that the binding affinity of PATD to ASBT is strong enough to be compared with the affinity of natural bile acid due to its oligomeric bile acid moiety. The possibility of tetraDOCA binding to the hydrophobic cavity in ASBT increased the molecular interaction between PATD and ASBT.

Computer Simulation of PATD and ASBT. The development of bile acid transporter inhibitors can be stimulated by revealing the 3D structure of targets. The recently reported molecular structure of ASBT shows that bile acids fit into a tight pocket with the steroid nucleus in the ligand-binding domain of ASBT.[16] The overall space of the pocket allows simultaneous binding of 3 to 4 bile acid molecules to the hydrophobic groove of ASBT, thereby inducing high binding affinity between the tetramer of deoxycholic acid and ASBT (Figure 1). The bile acid-binding cavity in ASBT is open to the cytoplasm and is approximately 1008 Å^3 in size, meaning it is much bigger than the size of a bile acid (150−250 Å^3).[40] Therefore, it is necessary to use an oligomeric hydrophobic substrate, tetraDOCA, for strong ASBT binding. Computer docking simulation using poly(acrylic acid) fragment and tetraDOCA demonstrated that the molecular structure of the polymer did not sterically hinder the binding of tetraDOCA to ASBT.

Molecular simulation plays an efficient role in the field of drug design and development by docking toward the active binding site of targets. We used a poly(acrylic acid) fragment for simulation due to its huge molecular size, and Autodock v 1.0.3 calculated the energy of binding. The minimum internal binding energy of poly(acrylic acid)−tetraDOCA that conjugate in ASBT was −9.2 kcal/mol, which indicated tetraDOCA could bind to ASBT. The binding energy of taurocholic acid, deoxycholic acid, or other natural bile acid ranged between −6.2 and −9.0 kcal/mol. Molecular dynamics (MD) simulation of PATD and ASBT was carried out using the Discovery Studio program and the CHARMM force field, which can describe biological macromolecules such as proteins, nucleic acids, and their ligands in aqueous environment. The binding interaction between PATD and ASBT is strong and more stable than the interaction of poly(acrylic acid) and ASBT. We also measured the interaction energy of the PATD-ASBT and poly(acrylic acid)−ASBT complex during the MD simulation (Figure 2). In the docking structure, the conformation of tetraDOCA in ASBT did not change after MD simulation. The maintained interaction energy of complex also supported this finding, which indicated that tetrameric bile acid could form a stable binding pose in the binding pocket of bile acid transporter. Recent studies have shown that the kinetics of drug−receptor binding could be important in drug discovery and development.[41−43] In our study, PATD not only showed a strong molecular interaction with ASBT in SPR, but also exhibited prolonged molecular dynamics in computer

DOI: 10.1021/acs.bioconjchem.5b00230
Bioconjugate Chem. 2015, 26, 1597−1605

dynamic simulation. When tetraDOCA and ASBT interact via hydrophobic and hydrophilic interactions, the complex tends to be kinetically stable due to the strong hydrophobicity of the bile acid.

Cellular Binding of PATDs. PATDs were studied regarding the ASBT binding efficiency, as well as its cellular action and toxicity as ASBT inhibitors. We carried out a cell binding and viability assay to confirm the cellular action of PATD using ASBT overexpressed MDCK cell line. At first, we transfected MDCK cells using the human ASBT gene (SLC10A2) to visualize the binding of PATD to ASBT on the cell surface in previous work.[44] ASBT overexpressed MDCK cells were incubated with fluorescence labeled poly(acrylic acid), PATD1, or PATD3. Green fluorescein image was detected on the surface of MDCK cells, and fluorescence conjugated poly(acrylic acid) did not show any significant differences in MDCK-ASBT cells (Figure 3). This demonstrated that overexpressed ASBT could react with PATD1 or PATD3 forming a PATD-ASBT complex, followed by the inhibition of ASBT activity. Molecular mechanism studies including colocalization and natural ligand inhibition test for tetraDOCA were conducted in previous study in detail.[37,44] In addition, the viability test was carried out to check the toxicity of PATD1 or PATD3 on cells. The cell viability assay using CCK-8 confirmed no cytotoxicity when PATD1 or PATD3 was administered up to 400 μg/mL. Viability of MDCK cells was decreased by 8% at the maximum dose. Through this process we created, we were able to conclude that PATD can interact with ASBT in the ileum without toxicity.

Animal Study Using PATDs. We evaluated the therapeutic effect of PATD in vivo using HFD feeding, which when induced in animals, can cause obesity and leading to metabolic disorders. In the HFD-fed mice, hypercholesterolemia and hepatic fat accumulation were induced to evaluate the therapeutic effect of PATD. To evaluate the therapeutic effect of PATD1 and PATD3 in vivo, PATDs were administered to HFD fed mice. Feeding HFD increased the body weight gain in the control or PATD-treated group (Figure 4A). After 13 weeks, the body weights were increased by 154.2 ± 10.9% (ND-feeding group), 260.8 ± 13.7% (HFD-feeding group), 240.2 ± 15.6% (HFD-feeding + PATD1 treatment), and 237.0 ± 13.1% (HFD-feeding + PATD3 treatment).

The PATD1 and PATD3 treatment reduced the body weight and liver weight gain in mice. In particular, the liver weight of the mice was significantly reduced by the treatment of PATDs (Figure 4B). In comparison with the liver weight of HFD-fed mice, the treatment with 10 mg/kg PATD1 or PATD3 per day for 9 weeks resulted in a reduction of the liver weight by −27.3% or −40.9%, respectively. This result indicates that the reduced liver weight gain is related to the decreased body weight of the PATD treated group (PATD1 or PATD3 treatment: the reduced fat accumulation in the liver, which was visualized by oil red O staining). HFD-fed mice exhibited sufficient fat accumulation in Oil red O staining and the images showed a successful increase in hepatic fat accumulation in HFD-fed mice (Figure 5). PATD treatment and inhibiting hepatic fat accumulation resulted in the inhibition of body weight gain. The amount of reduced fat accumulation in the liver verified the therapeutic effect of PATDs. In addition, a toxicity study for the ileum and blood concentration analysis were conducted; PATD showed no toxicity and low availability (Supporting Information).

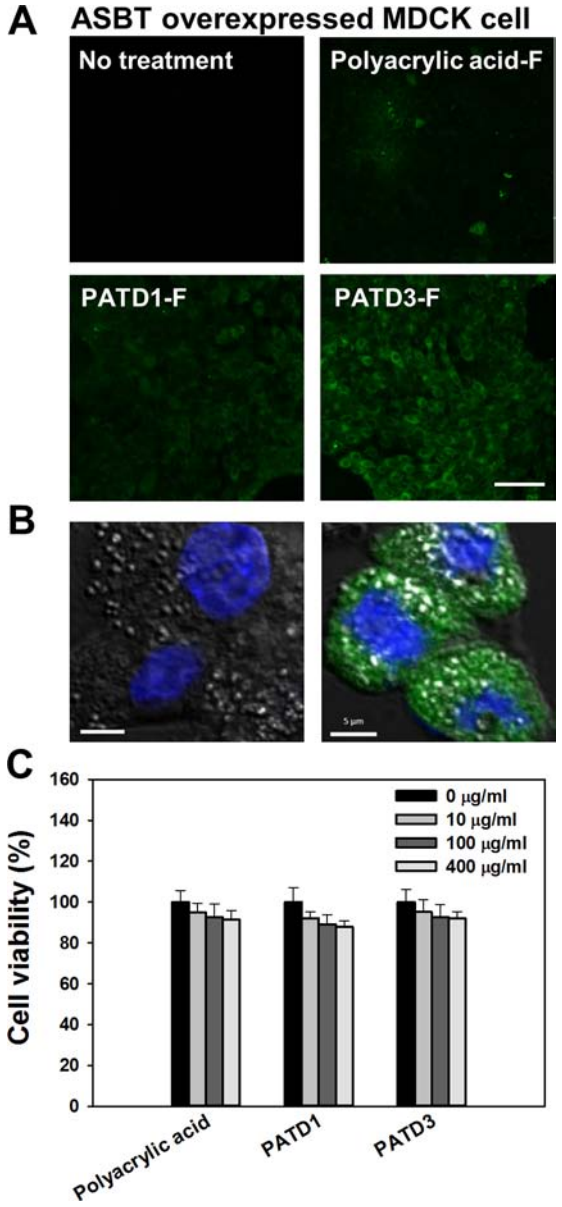

Figure 3. (A) Comparison of cellular binding of poly(acrylic acid) and PATD in ASBT overexpressed MDCK cells (200×). Scale bar = 50 μm. (B) Representative confocal image of Fluorosence (F)-labeled materials in MDCK-ASBT cells was compared to that in the untreated cells (800×). Scale bar = 5 μm. (C) Cell viability was maintained in the presence of low or high dose of PATDs (n = 7).

Since cholesterol is balanced by entero-hepatic circulation through bile acid synthesis and reabsorption, the inhibition of bile acid reuptake in the intestine decreases total cholesterol in the liver and the blood. In the result of the blood analysis, PATDs significantly decreased total cholesterol (TC) and triglyceride (TG) contents in the plasma (Figure 6). Among the different risk factors for dyslipidemia, a increase in LDL level appears to primarily indicate that high LDL concentrations promote atherosclerosis. The plasma level of low density cholesterol (LDL) was lower than that of the control group, thereby decreasing the atherogenic index in the PATD3 treated group (Figure 6C). High plasma level of LDL and hepatic fat accumulation have been associated with other metabolic abnormalities like glucose tolerance. Fasting glucose was monitored in the plasma and an oral glucose tolerance test

DOI: 10.1021/acs.bioconjchem.5b00230
Bioconjugate Chem. 2015, 26, 1597−1605

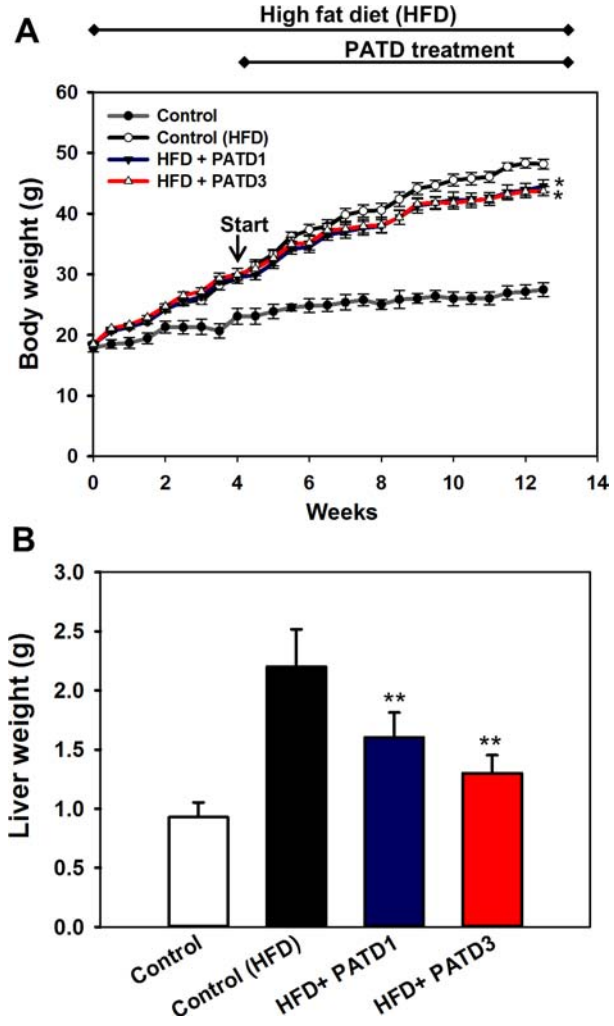

Figure 4. Body wight and liver weight gain in high fat diet experimental model (A) Effect of PATD on body weight gain in mice. Male C57BL/6 mice were fed either a normal diet (ND) or a high-fat diet (HFD) for 13 weeks (n = 7). For 9 weeks of diet feeding, PATD1 and PATD3 (10 mg/kg/day) were orally administered to mice after being fasted for 4 h. (B) Changes in the liver weight. By reducing the weight of the liver, PATD inhibited body weight gain. *p < 0.05 vs control group (HFD), **p < 0.001 vs control group (HFD).

(OGTT) was carried out on the last day of high-fat diet experiment (Figure 6D). In OGTT, the blood glucose level of HFD-fed group rapidly increased to 522 mg/dL within 15 min. In contrast, the blood glucose level of PATD3 group reached the highest concentration (419 mg/dL) after 15 min of glucose injection and then gradually decreased afterward, showing that PATD treatment prevented a rapid increase of blood glucose level and decreased the glucose level rapidly (Figure 6E). These results demonstrate that PATD treatment on the HFD animal group results in the inhibition of both hyperlipidemia and hepatic fat accumulation.

CONCLUSION

We developed a new polymer based biomaterial for the inhibition of ASBT and manifesting hypocholesterolemic effect for the treatment of hypercholesterolaemia. PATD effectively bound to ASBT in SPR and ASBT overexpressed MDCK cells without any cytotoxicity. We evaluated the therapeutic effect of PATD in an HFD-induced hyperlipidemia animal model, and the results showed that PATD3 prevented hyperlipidemia and hepatic fat accumulation. These findings, thus, strengthen the notion that bile acid and polymer based biomaterials can be utilized as potent ASBT inhibitors when interacting with their transporters.

MATERIALS AND METHODS

Materials. Deoxycholic acid (DOCA), *N*-hydroxylsuccinimide (NHS), 1-ethyl-3-(3-(dimethylamino)propyl)-carbodiimide (EDAC), ethylene-diamine, fluoresceinamine, and poly(acrylic acid) (PAA) were purchased from Sigma Chemical Co. (St. Louis, MO). Anhydrous dimethyl sulfoxide (DMSO) and acetone were obtained from Daejung Chemicals and Metals Co. (Shiheung, South Korea). Polyethylene polyoxypropylene block copolymer (poloxamer) was purchased from BASF (Ludwigshafen, Germany) and caprylocaproyl macrogolglyceride (Labrasol) was obtained from Gattefossé (Lyon, France). Cell counting kit (CCK-8) was purchased from Dojindo molecular technologics. All chemicals were used without further purification.

Synthesis of PATD. PATDs were synthesized by coupling reaction of poly(acrylic acid) and tetraDOCA, as shown in Figure 1. Polyacrylic acid (average molecular weight, 100 kDa) was reacted with tetraDOCA in DMF/FA solution for 12 h using 1-ethyl-3-(3-(dimethylamino)propyl)carbodiimide (EDAC) and *N*-hydroxylsuccinimide (NHS). The feed molecular ratio of reaction was described in Table 1. Unreacted EDAC, HOSu, and tetraDOCA were removed by dialysis for 48 h in methanol/water solution using a membrane of MWCO 8000 Da and then confirmed by TLC.

TetraDOCA was synthesized following the procedure described in the previous study.[37] Briefly, lysine dimer, Boc-CH_3O-Lys(Lys(Boc)$_2$), was synthesized using lysine peptides in DMF and then purified. Using lysine dimer, lysine trimer was synthesized and purified by column chromatography (10% MeOH/MC as an eluent). In another batch, DOCA was activated using the DCC/NHS coupling method.[45] After a deprotection process, lysine trimer was reacted with activated DOCA-NHS. To introduce an amine group to tetraDOCA−lysine peptide conjugate, the conjugate was reacted with EDA for 48 h, and purified by column chromatography. The final compound, named tetraDOCA, was confirmed by TLC and MALDI-TOF (Voyager-DE STR Biospectrometry Workstation, Applied Biosystems Inc.).

Characterization. The average conjugated ratios of tetraDOCA to poly(acrylic acid) were determined by the sulfuric acid method which was introduced in a previous study.[46] Briefly, poly(acrylic acid) , poly(acrylic acid)−tetraDOCA mixtures, and poly(acrylic acid)−tetraDOCA conjugates were dissolved in water (140 μL) and mixed with sulfuric acid solution (360 μL) at 70 °C for 30 min and then cooled. The absorbance was measured at 420 nm using UV/vis spectrometer, and the conjugation ratio was calculated. Then, we measured the binding affinities of a bile acid (taurocholic acid; TCA), poly(acrylic acid) , and PATD to ASBT using BIAcore T100 (GE Healthcare, Uppsala, Sweden). In surface plasmon resonance (SPR) study, the samples were prepared at concentrations ranging from 1 to 0.0078 μM and the running solution was 2% DMSO containing HEPES buffer supplemented with 150 mM NaCl. Recombinant human ASBT was immobilized onto a sensor chip CM5 using DMSO, EDAC, and NHS, then measurements were performed at a flow rate of 20 μL/min. Biacore T100 Evaluation software was used to

DOI: 10.1021/acs.bioconjchem.5b00230
Bioconjugate Chem. 2015, 26, 1597−1605

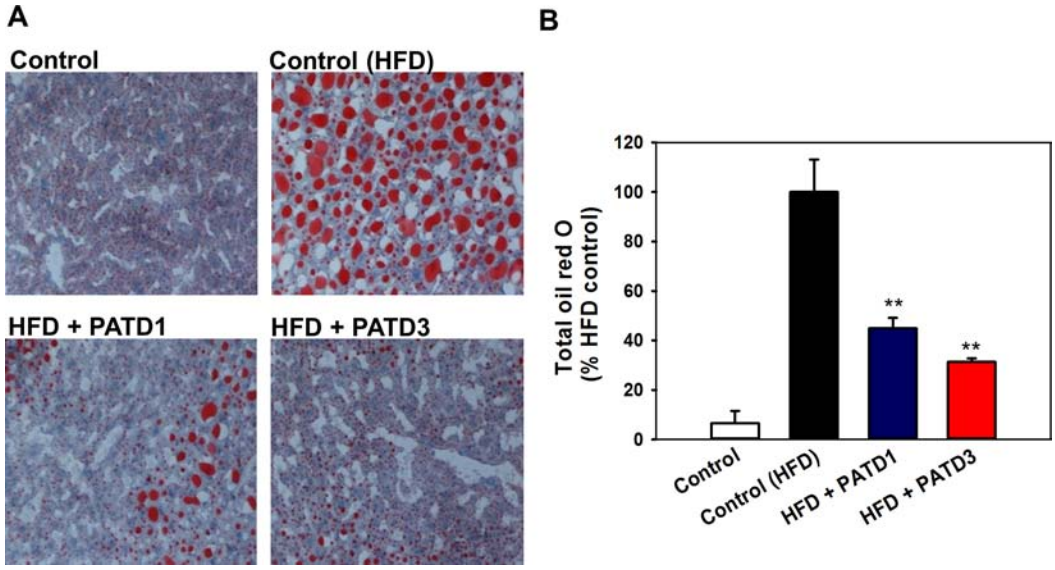

Figure 5. Inhibition of liver fat accumulation by PATD. (A) Oil red O staining of the liver in mice that were fed an ND, HFD or HFD with PATDs. PATD treatment significantly reduced fat accumulation in the liver. (B) Analyses of oil red O staining with *ImageJ* software ($n = 5$) *$p < 0.05$ vs control group (HFD), **$p < 0.001$ vs control group (HFD).

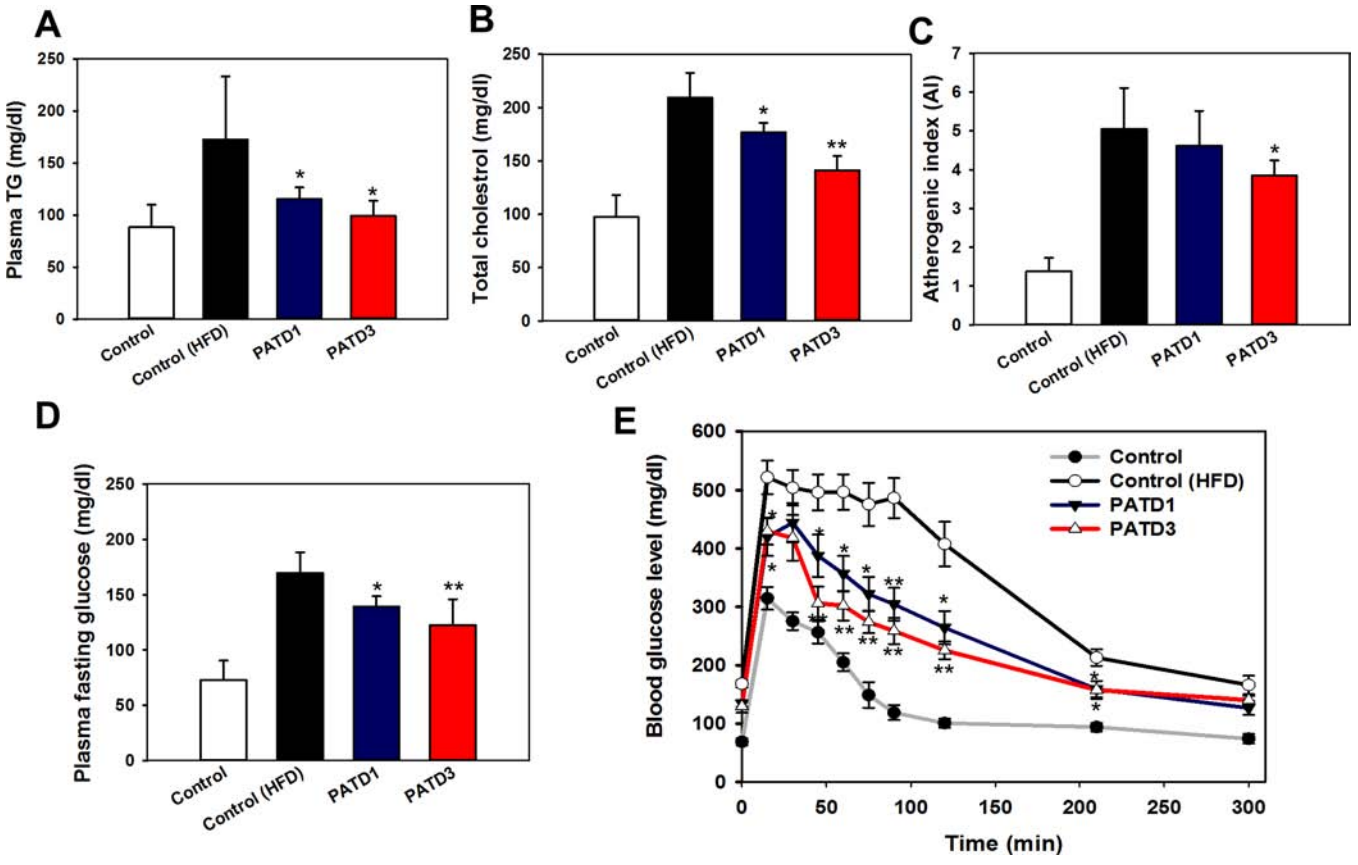

Figure 6. Therapeutic effect of PATD in HFD-fed mice. (A) Plasma Triglyceride (TG). (B) Plasma Total cholesterol (TC). (C) Atherogenic index. (D) Plasma fasting glucose. (E) Oral glucose tolerance test (OGTT). *$p < 0.05$ vs control group (HFD), **$p < 0.001$ vs control group (HFD).

calculate the affinity of samples to ASBT as described in Table 1.

Molecular Dynamic Simulation. The crystal structure of ASBT (protein data bank [PDB] code, 3ZUX and 3ZUY) was already reported.[40] The molecular structure of ASBT (3ZUX) without the bound taurocholic acid (TCA) and lipid molecules was used for the docking and dynamic simulation. The molecular docking simulation was performed using the AutoDock v 1.0.3 program with default parameters.[47] Illustrations of the 3D model were generated and visualized using the PyMol program. Molecular dynamic simulations were performed using Discovery Studio 3.0 with the CHARMm

DOI: 10.1021/acs.bioconjchem.5b00230
Bioconjugate Chem. 2015, 26, 1597−1605

(Chemistry at HARvard Molecular Mechanics) force field.[48] Briefly, ASBT complex was generated and solvated with the water molecules in an explicit spherical boundary condition. Each simulation was carried out by Standard Dynamics Cascade protocol of Discovery Studio 3.0 which consists of minimization, equilibrium, and run steps. Constant temperature and constant-volume ensemble (NVT) was selected. The molecular movements of polyacrylic acid and tetraDOCA were recorded every 500 ns. Molecular dynamic simulation steps were carried out in the Generalized Born with a simple SWitching (GBSW) implicit solvent model for application of the solvent (water) effect.

Binding and Viability Study Using ASBT Overexpressed MDCK Cell. Madin-Darby canine kidney (MDCK) cell line obtained from the Korea Cell Bank (Korea) and was transfected using SLC10A2 (sodium/bile acid co-transporter family) human cDNA open reading frame (ORF) clone and Lipofectamine 2000.[37] ASBT overexpressed MDCK cells were cultured in DMEM high glucose medium (GIBCO, Invitrogen, CA) supplemented with 10% (v/v) FBS (GIBCO, Invitrogen, CA) and penicillin−streptomycin. To evaluate cellular binding of materials, fluorescence labeled poly(acrylic acid) and PATDs were synthesized and treated to the cells. Briefly, they were prepared by conjugation between the primary amine of fluoresceinamine and the carboxylic group of acrylic acid in water/DMF using EDAC/NHS. After synthesis, they were purified by dialysis in methanol/water solution using a membrane of MWCO 8000 Da. MDCK-ASBT cells were incubated with fluorescence-labeled materials in sodium chloride (200 mM) containing HBSS medium at 37 °C for 1 h. After repeated washing steps, cells were fixed using 4% cold paraformaldehyde for 10 min. The nuclei were stained by Hoechst, and images were acquired with a confocal laser scanning microscopy (CLSM).

The viability of drug treated cells was measured by a cell counting kit (CCK-8). Cells suspended in 100 μL of DMEM high glucose medium were added into a 96-well culture plate and were incubated for 24 h. When cells reached confluence, we treated cells with the synthesized materials at different concentrations (n = 7). After 6 h, 10 μL of CCK (WST-8) solution was added into each well. The absorbance was measured at 450 nm wavelength using a microplate reader after 1 h incubation.

Animal Study Using High-Fat Diet (HFD). All procedures for animal experiments were approved by the Committee of the Use and Care on Animals according to the regulations of the Institutional Animal Ethics Committee of the Seoul National University animal care facility. To investigate the therapeutic potential of PATD, 7-week-old male C57BL/6 mice were obtained from Orient Bio Inc. (Seungnam, South Korea) and were acclimatized for 1 week. The mice were fed either a normal diet (ND) or an HFD (60% of kilocalories as fat, Research Diets) for 13 weeks.[49] HFD-fed animals were randomly assigned into three groups when we started PATD treatment (n = 7). In the PATD treated group, PATD1 or PATD3 (10 mg/kg/day) in an oral formulation containing labrasol and Poloxamer 188 as solubilizers was orally administered to the mice. The mice were fasted for 4 h before administering PATDs.

Oil Red O Staining. For oil red O staining, animals were sacrificed after the high-fat diet experiment. The left lateral lobe of the liver was sliced and frozen. The samples were cut into 4 μm sections and then affixed to microscope slides (n = 5). The liver sections were stained in fresh oil red O for 10 min and rinsed in water. After the oil red O treatment, the sections were observed using a microscope (Eclipse TE2000S, Nikon, Japan) within 4 h and analyzed with *ImageJ* (NIH software).

Analysis of Blood Samples and Oral Glucose Tolerance Test. Blood (400 μL) was collected from mice after sacrifice (n = 7). Plasma triglyceride (TG) and total cholesterol (TC) were measured using a FUJI DRI-CHEM3500 (FUJIFILM, Tokyo, Japan). The atherosclerotic index (AI) was calculated as (total cholesterol − high density lipoprotein cholesterol)/(high density lipoprotein cholesterol). Oral glucose tolerance test (OGTT) was carried out to measure the glucose responsiveness on the last day of the high-fat diet experiment. Each group was fasted for 16 h before the oral treatment of glucose solution (2 g/kg). The blood glucose level in the blood was measured using a glucometer (Super glucocard II) at 0, 15, 30, 45, 60, 75, 90, 120, 210, and 300 min after oral glucose treatment (n = 7).

Statistical Analysis. All results were analyzed by comparing the means of groups in in vitro and in vivo experiments using one-way analyses of variance (ANOVA) followed by Bonferroni's posthoc tests using Sigmaplot 12. p-Values less than 0.05 were considered to be statistically significant.

■ ASSOCIATED CONTENT

Ⓢ Supporting Information

PK study of PATD3; H&E tissue analysis in high-dose PATD3 treated mouse. The Supporting Information is available free of charge on the ACS Publications website at DOI: 10.1021/acs.bioconjchem.5b00230.

■ AUTHOR INFORMATION

Corresponding Author

*E-mail: yrbyun@snu.ac.kr. Tel: +82-2-880-7866. Fax: +82-2-872-7864.

Notes

The authors declare no competing financial interest.

■ ACKNOWLEDGMENTS

This study was supported by grants from the Bio & Medical Technology Development Program (grant no. 2012028833) and Basic Science Research Program (grant no. 2010-0027955) of the National Research Foundation of Korea (NRF) funded by Korean Ministry of SIP[MSIP]. The authors thank National Center for Inter-University Research Facilities for technical assistance.

■ ABBREVIATIONS

ASBT, apical sodium-dependent bile acid transporter; HFD, high-fat diet; PATD, poly(acrylic acid)−tetraDOCA conjugate; TCA, taurocholic acid

■ REFERENCES

(1) Ross, R., and Harker, L. (1976) Hyperlipidemia and atherosclerosis. *Science 193*, 1094−100.

(2) Drechsler, M., Megens, R. T., van Zandvoort, M., Weber, C., and Soehnlein, O. (2010) Hyperlipidemia-triggered neutrophilia promotes early atherosclerosis. *Circulation 122*, 1837−45.

(3) Hansson, G. K., and Libby, P. (2006) The immune response in atherosclerosis: a double-edged sword. *Nat. Rev. Immunol. 6*, 508−19.

(4) Zhou, X., Levin, E. J., Pan, Y., McCoy, J. G., Sharma, R., Kloss, B., Bruni, R., Quick, M., and Zhou, M. (2014) Structural basis of the

DOI: 10.1021/acs.bioconjchem.5b00230
Bioconjugate Chem. 2015, 26, 1597−1605

alternating-access mechanism in a bile acid transporter. *Nature 505*, 569−73.
(5) Javitt, N. B. (1994) Bile acid synthesis from cholesterol: regulatory and auxiliary pathways. *FASEB J. 8*, 1308−11.
(6) Hofmann, A. F. (2009) The enterohepatic circulation of bile acids in mammals: form and functions. *Front. Biosci., Landmark Ed. 14*, 2584−98.
(7) Roberts, M. S., Magnusson, B. M., Burczynski, F. J., and Weiss, M. (2002) Enterohepatic circulation: physiological, pharmacokinetic and clinical implications. *Clin. Clin. Pharmacokinet. 41*, 751−90.
(8) Xu, G., Pan, L. X., Erickson, S. K., Forman, B. M., Shneider, B. L., Ananthanarayanan, M., Li, X., Shefer, S., Balasubramanian, N., Ma, L., et al. (2002) Removal of the bile acid pool upregulates cholesterol 7α-hydroxylase by deactivating FXR in rabbits. *J. Lipid. Res. 43*, 45−50.
(9) Sakamoto, S., Kusuhara, H., Miyata, K., Shimaoka, H., Kanazu, T., Matsuo, Y., Nomura, K., Okamura, N., Hara, S., Horie, K., et al. (2007) Glucuronidation converting methyl 1-(3,4-dimethoxyphenyl)-3-(3-ethylvaleryl)-4-hydroxy-6,7,8-trimethoxy-2-naphthoate (S-8921) to a potent apical sodium-dependent bile acid transporter inhibitor, resulting in a hypocholesterolemic action. *J. Pharmacol. Exp. Ther. 322*, 610−8.
(10) Kobayashi, M., Ikegami, H., Fujisawa, T., Nojima, K., Kawabata, Y., Noso, S., Babaya, N., Itoi-Babaya, M., Yamaji, K., Hiromine, Y., et al. (2007) Prevention and treatment of obesity, insulin resistance, and diabetes by bile acid-binding resin. *Diabetes 56*, 239−47.
(11) Lewis, M. C., Brieaddy, L. E., and Root, C. (1995) Effects of 2164U90 on ileal bile acid absorption and serum cholesterol in rats and mice. *J. Lipid. Res. 36*, 1098−105.
(12) Bhat, B. G., Rapp, S. R., Beaudry, J. A., Napawan, N., Butteiger, D. N., Hall, K. A., Null, C. L., Luo, Y., and Keller, B. T. (2003) Inhibition of ileal bile acid transport and reduced atherosclerosis in apoE−/− mice by SC-435. *J. Lipid. Res. 44*, 1614−21.
(13) Root, C., Smith, C. D., Sundseth, S. S., Pink, H. M., Wilson, J. G., and Lewis, M. C. (2002) Ileal bile acid transporter inhibition, CYP7A1 induction, and antilipemic action of 264W94. *J. Lipid Res. 43*, 1320−30.
(14) Downes, M., Verdecia, M. A., Roecker, A. J., Hughes, R., Hogenesch, J. B., Kast-Woelbern, H. R., Bowman, M. E., Ferrer, J. L., Anisfeld, A. M., Edwards, P. A., et al. (2003) A chemical, genetic, and structural analysis of the nuclear bile acid receptor FXR. *Mol. Cell 11*, 1079−92.
(15) Hambruch, E., Miyazaki-Anzai, S., Hahn, U., Matysik, S., Boettcher, A., Perovic-Ottstadt, S., Schluter, T., Kinzel, O., Krol, H. D., Deuschle, U., et al. (2012) Synthetic farnesoid X receptor agonists induce high-density lipoprotein-mediated transhepatic cholesterol efflux in mice and monkeys and prevent atherosclerosis in cholesteryl ester transfer protein transgenic low-density lipoprotein receptor (−/−) mice. *J. Pharmacol. Exp. Ther. 343*, 556−67.
(16) Schaap, F. G., Trauner, M., and Jansen, P. L. M. (2014) Bile acid receptors as targets for drug development. *Nat. Rev. Gastroenterol. Hepatol. 11*, 55−67.
(17) Pellicciari, R., Fiorucci, S., Camaioni, E., Clerici, C., Costantino, G., Maloney, P. R., Morelli, A., Parks, D. J., and Willson, T. M. (2002) 6α-Ethyl-chenodeoxycholic acid (6-ECDCA), a potent and selective FXR agonist endowed with anticholestatic activity. *J. Med. Chem. 45*, 3569−72.
(18) Pellicciari, R., Gioiello, A., Macchiarulo, A., Thomas, C., Rosatelli, E., Natalini, B., Sardella, R., Pruzanski, M., Roda, A., Pastorini, E., et al. (2009) Discovery of 6α-ethyl-23(S)-methylcholic acid (S-EMCA, INT-777) as a potent and selective agonist for the TGR5 receptor, a novel target for diabesity. *J. Med. Chem. 52*, 7958−61.
(19) Gracia-Sancho, J., Hernandez-Gea, V., and Garcia-Pagan, J. C. (2014) Obeticholic acid: a new light in the shadows treating portal hypertension? *Hepatology 59*, 2072−3.
(20) Mudaliar, S., Henry, R. R., Sanyal, A. J., Morrow, L., Marschall, H. U., Kipnes, M., Adorini, L., Sciacca, C. I., Clopton, P., Castelloe, E., et al. (2013) Efficacy and safety of the farnesoid X receptor agonist obeticholic acid in patients with type 2 diabetes and nonalcoholic fatty liver disease. *Gastroenterology 145*, 574−82 e1.
(21) Abel, U., Schluter, T., Schulz, A., Hambruch, E., Steeneck, C., Hornberger, M., Hoffmann, T., Perovic-Ottstadt, S., Kinzel, O., Burnet, M., et al. (2010) Synthesis and pharmacological validation of a novel series of non-steroidal FXR agonists. *Bioorg. Med. Chem. Lett. 20*, 4911−7.
(22) Claudel, T., Staels, B., and Kuipers, F. (2005) The Farnesoid X receptor: a molecular link between bile acid and lipid and glucose metabolism. *Arterioscler., Thromb., Vasc. Biol. 25*, 2020−30.
(23) Wang, Y. D., Chen, W. D., Moore, D. D., and Huang, W. (2008) FXR: a metabolic regulator and cell protector. *Cell Res. 18*, 1087−95.
(24) Pircher, P. C., Kitto, J. L., Petrowski, M. L., Tangirala, R. K., Bischoff, E. D., Schulman, I. G., and Westin, S. K. (2003) Farnesoid X receptor regulates bile acid-amino acid conjugation. *J. Biol. Chem. 278*, 27703−11.
(25) Watanabe, M., Houten, S. M., Mataki, C., Christoffolete, M. A., Kim, B. W., Sato, H., Messaddeq, N., Harney, J. W., Ezaki, O., Kodama, T., et al. (2006) Bile acids induce energy expenditure by promoting intracellular thyroid hormone activation. *Nature 439*, 484−9.
(26) Thomas, C., Gioiello, A., Noriega, L., Strehle, A., Oury, J., Rizzo, G., Macchiarulo, A., Yamamoto, H., Mataki, C., Pruzanski, M., et al. (2009) TGR5-mediated bile acid sensing controls glucose homeostasis. *Cell Metab.*, 167−77.
(27) Li, T., Holmstrom, S. R., Kir, S., Umetani, M., Schmidt, D. R., Kliewer, S. A., and Mangelsdorf, D. J. (2011) The G protein-coupled bile acid receptor, TGR5, stimulates gallbladder filling. *Mol. Endocrinol. 25*, 1066−71.
(28) Pols, T. W., Nomura, M., Harach, T., Lo Sasso, G., Oosterveer, M. H., Thomas, C., Rizzo, G., Gioiello, A., Adorini, L., Pellicciari, R., et al. (2011) TGR5 activation inhibits atherosclerosis by reducing macrophage inflammation and lipid loading. *Cell Metab.*, 747−57.
(29) Wu, Y., Aquino, C. J., Cowan, D. J., Anderson, D. L., Ambroso, J. L., Bishop, M. J., Boros, E. E., Chen, L., Cunningham, A., Dobbins, R. L., et al. (2013) Discovery of a highly potent, nonabsorbable apical sodium-dependent bile acid transporter inhibitor (GSK2330672) for treatment of type 2 diabetes. *J. Med. Chem. 56*, 5094−114.
(30) Cowan, D. J., Collins, J. L., Mitchell, M. B., Ray, J. A., Sutton, P. W., Sarjeant, A. A., and Boros, E. E. (2013) Enzymatic- and iridium-catalyzed asymmetric synthesis of a benzothiazepinylphosphonate bile acid transporter inhibitor. *J. Org. Chem. 78*, 12726−34.
(31) Zhang, Y., Chan, H. F., and Leong, K. W. (2013) Advanced materials and processing for drug delivery: The past and the future. *Adv. Drug Delivery Rev. 65*, 104−120.
(32) Sedo, J., Saiz-Poseu, J., Busque, F., and Ruiz-Molina, D. (2013) Catechol-Based Biomimetic Functional Materials. *Adv. Mater. 25*, 653−701.
(33) Lopez-Jaramillo, F. J., Giron-Gonzalez, M. D., Salto-Gonzalez, R., Hernandez-Mateo, F., and Santoyo-Gonzalez, F. (2015) In vitro and in vivo evaluation of novel cross-linked saccharide based polymers as bile acid sequestrants. *Molecules 20*, 3716−29.
(34) Park, J. K., Kim, T. H., Nam, J. P., Park, S., Park, Y., Jang, M. K., and Nah, J. W. (2014) Bile acid conjugated chitosan oligosaccharide nanoparticles for paclitaxel carrier. *Macromol. Res. 22*, 310−317.
(35) Duan, H., Ning, M., Zou, Q., Ye, Y., Feng, Y., Zhang, L., Leng, Y., and Shen, J. (2015) Discovery of intestinal targeted TGR5 agonists for the treatment of type 2 diabetes. *J. Med. Chem. 58*, 3315−3328.
(36) Sakanaka, T., Inoue, T., Yorifuji, N., Iguchi, M., Fujiwara, K., Narabayashi, K., Kakimoto, K., Nouda, S., Okada, T., Kuramoto, T., et al. (2015) The effects of a TGR5 agonist and a dipeptidyl peptidase IV inhibitor on dextran sulfate sodium-induced colitis in mice. *J. Gastroenterol. Hepatol. 30* (Suppl 1), 60−5.
(37) Al-Hilal, T. A., Park, J., Alam, F., Chung, S. W., Park, J. W., Kim, K., Kwon, I. C., Kim, I. S., Kim, S. Y., and Byun, Y. (2014) Oligomeric bile acid-mediated oral delivery of low molecular weight heparin. *J. Controlled Release 175*, 17−24.
(38) Alam, F., Al-Hilal, T. A., Chung, S. W., Seo, D., Mahmud, F., Kim, H. S., Kim, S. Y., and Byun, Y. (2014) Oral delivery of a potent

DOI: 10.1021/acs.bioconjchem.5b00230
Bioconjugate Chem. 2015, 26, 1597−1605

anti-angiogenic heparin conjugate by chemical conjugation and physical complexation using deoxycholic acid. *Biomaterials 35*, 6543−52.
(39) Al-Hilal, T. A., Alam, F., and Byun, Y. (2013) Oral drug delivery systems using chemical conjugates or physical complexes. *Adv. Drug Delivery Rev. 65*, 845−64.
(40) Hu, N. J., Iwata, S., Cameron, A. D., and Drew, D. (2011) Crystal structure of a bacterial homologue of the bile acid sodium symporter ASBT. *Nature 478*, 408−11.
(41) Lu, H., and Tonge, P. J. (2010) Drug-target residence time: critical information for lead optimization. *Curr. Opin. Chem. Biol. 14*, 467−74.
(42) Copeland, R. A., Pompliano, D. L., and Meek, T. D. (2006) Drug-target residence time and its implications for lead optimization. *Nat. Rev. Drug Discovery 5*, 730−9.
(43) Pan, A. C., Borhani, D. W., Dror, R. O., and Shaw, D. E. (2013) Molecular determinants of drug-receptor binding kinetics. *Drug Discovery Today 18*, 667−73.
(44) Al-Hilal, T. A., Chung, S. W., Alam, F., Park, J., Lee, K. E., Jeon, H., Kim, K., Kwon, I. C., Kim, I. S., Kim, S. Y., et al. (2014) Functional transformations of bile acid transporters induced by high-affinity macromolecules. *Sci. Rep. 4*, 4163.
(45) Lee, Y., Nam, J. H., Shin, H. C., and Byun, Y. (2001) Conjugation of low-molecular-weight heparin and deoxycholic acid for the development of a new oral anticoagulant agent. *Circulation 104*, 3116−20.
(46) Nichifor, M., and Carpov, A. (1999) Bile acids covalently bound to polysaccharides 1. Esters of bile acids with dextran. *Eur. Polym. J. 35*, 2125−2129.
(47) Trott, O., and Olson, A. J. (2010) AutoDock Vina: improving the speed and accuracy of docking with a new scoring function, efficient optimization, and multithreading. *J. Comput. Chem. 31*, 455−61.
(48) MacKerell, A. D. (1998) Developments in the CHARMM all-atom empirical energy function for biological molecules. *Abstr. Pap. Am. Chem. Soc. 216*, U696−U696.
(49) Kim, Y. W., Kim, Y. M., Yang, Y. M., Kim, T. H., Hwang, S. J., Lee, J. R., Kim, S. C., and Kim, S. G. (2010) Inhibition of SREBP-1c-mediated hepatic steatosis and oxidative stress by sauchinone, an AMPK-activating lignan in Saururus chinensis. *Free Radic. Biol. Med. 48*, 567−578.

DOI: 10.1021/acs.bioconjchem.5b00230
Bioconjugate Chem. 2015, 26, 1597−1605